www.amlett.com, www.vbripress.com/aml DOI: 10.5185/amlett.2014.592 Published online by the VBRI press in 2014

Effect of catalyst concentration on the synthesis of MWCNT by single step pyrolysis

B. V. Mohan Kumar[1,3], Rajesh Thomas[2], Ambily Mathew[2], G. Mohan Rao[2], D. Mangalaraj[1], N. Ponpandian[1], C. Viswanathan[1*]

[1]*Department of Nanoscience & Technology, Bharathiar University, Coimbatore 641 046, India*
[2]*Department of Instrumentation & Applied Physics, Indian Institute of Science, Bangalore 560 012, India*
[3]*Government First Grade College, K.R. Pura, Bangalore 560 036, India*

[*]Corresponding author. Tel: (+91) 422 2428422, Fax: (+91) 422 2422387; E-mail: viswanathan@buc.edu.in

Received: 22 February 2014, Revised: 23 June 2014 and Accepted: 28 June 2014

ABSTRACT

Multiwall carbon nanotubes (MWCNT) are synthesised by cost effective method of pyrolysing xylene (as hydrocarbon, precursor) in the presence of ferrocene (as catalyst) at 750°C. The so obtained MWCNTs has a length ranging from 90 µm to 300 µm and diameter ranging from 20 nm to 200 nm depending on the amount of ferrocene added to the xylene for the synthesis. The diameter of the MWCNT's increased with the increase in ferrocene content in the precursor solution. Bigger agglomerates of iron particle lead to the growth of larger diameter MWCNTs. These MWCNTs with higher concentration of iron nanoparticles in it are useful for catalytic applications. X-ray diffraction (XRD) of the as-synthesised MWCNTs showed a graphitic-like peak (002). Field emission scanning electron microscope (FESEM) is utilized for its morphological analysis, Raman analysis showed the presence of D band ($\approx$1350 cm^{-1}) and G band ($\approx$1580 cm^{-1}) indicating high crystalline graphitic layers. Fourier transform infrared (FTIR) studies in the transmission mode were carried out in the range 400 - 4000 cm^{-1} (peaks at 1386, 1639, 2363, 3434, 3747 cm^{-1} etc.) for bond stretching analysis. All the characterization processes were carried out before and after purification process. The MWCNT's diameter and their distribution are studied with the help of ImageJ software using the FESEM micrographs. Copyright © 2014 VBRI press.

Keywords: Multiwall carbon nanotubes; single step pyrolysis; ferrocene; xylene.

B. V. Mohan Kumar is an FIP research scholar under UGC scheme. At present he is graduate student in the department of Nanoscience & Technology, Bharathiar University, Coimbatore, India. His field of interest is in synthesis of carbon nanostructures and its applications to energy storage devices, batteries and biological applications.

Rajesh Thomas obtained his M.Sc., and M.Tech., from Barkathullah University, Bhopal, in 2006 and 2008 respectively. He joined as a graduate student in the dept. of Instrumentation and Applied Physics, Indian Institute of Science (IISc), and completed his Ph.D in material science in 2014. His field of interest is in energy storage devices, batteries, supercapacitors and carbon nanostructures.

C. Viswanathan, currently working as an assistant professor in Department of Nanoscience and Technology, Bharathiar University. He holds a M. Sc. and Ph. D. (2005) in physics from Bharathiar University and completed post doctoral position in University of Louis Pasteur at France and Marie Curie Post-Doctoral Fellow at Greece. His research interest involves nanostructing materials as a transducer for sensors and nanomaterials – based biosensor for pathogen and explosive detection.

Introduction

Ever since Iijima [**1**] discovered carbon nanotubes (CNT), there has been a tremendous development in the field of carbon nano world. Carbon nanotubes represent one of the most exciting research areas in the nanoscience and technology. These carbon nanostructures are stiffest and strongest fibers ever known with remarkable electronic, mechanical properties with potential applications in medicine, sensing devices and a host of other interesting

fields. The interesting characteristics arise due to the structure and the diameter of these carbon nanotubes.

MWCNTs are synthesised by various methods like by arc discharge, laser ablation, electrolysis, sonochemical or hydrothermal, chemical vapour deposition (CVD) methods and there are many more variants available in CVD like hot filament, water assisted, oxygen assisted, microwave plasma, radio frequency, thermal and plasma enhanced CVD to list a few [**2-4**]. With turpentine oil and ferrocene, vertically aligned N doped CNTs were synthesised by spray pyrolysis [**5**], with CCVD, MWCNTs were synthesised using Fe-supported NaX zeolite as the catalyst [**6**]. Thermal and electrochemical studies were done on vertically aligned CNTs grown by pyrolysis of camphor/ferrocene [**7**]. Vertically aligned CNTs composites were fabricated for membrane application using CVD [**8**]. The effect of temperature and catalyst concentration was studied on the growth of aligned CNTs [**9**]. Influence of ferrocene/benzene mole ratio on the carbon nanostructures grown by floating catalyst method has been reported [**10**]. Long and highly aligned CNTs were successfully grown by pyrolysis of ferrocene and acetylene [**11**]. MWCNTs growth is modelled using classical thermodynamics to explain the total carbon deposition as a function of time and temperature [**12**]. The effect of catalyst to carbon source ratio has been found to control the growth of vertically aligned CNTs on porous silicon templates [**13**]. Study of diameter and morphological dependence on experimental conditions during the growth of CNT arrays by spray pyrolysis has also been reported [**14**]. The different aspects like catalyst concentration, its effect on morphology, residual catalyst content, diameter distribution, defect density and oxidation resistance of MWCNTs by aerosol-assisted chemical vapour deposition has been studied for different hydrocarbons [**15**]. In this paper we report on the effect of catalyst concentration on the growth of MWCNTs by a simple method of single step pyrolysis process without using any carrier gas.

Experimental

Materials

All chemicals were bought with 99.9 percent purity (ferrocene from spectrochem Pvt., Ltd., Mumbai, xylene (sulphur free), HCl, HNO_3, H_2SO_4 from SD Fine-Chem Ltd., Mumbai) and used without any further purification. All the aqueous solutions were prepared with deionised water (Millipore), whose resistance is greater than 18 MΩ.

Synthesis of MWCNTs

Single step pyrolysis technique is employed for MWCNT synthesis [**16**]. This setup consists of a single stage tubular furnace unlike the double hot zone as in regular CVD and other methods [**17-19**]. The schematic diagram of the tubular furnace is shown in **Fig. 1**. The detailed experimental procedure of single stage furnace pyrolysis setup has been described elsewhere [**20**]. In brief, a mixture of ferrocene (as catalyst) and xylene (as hydrocarbon source) with certain catalyst to source ratio is taken in a quartz tube of length 70 cm and of inner diameter 1.2 cm whose one end is closed and the other open end is connected to a rubber bladder for the collection of reacted gases.

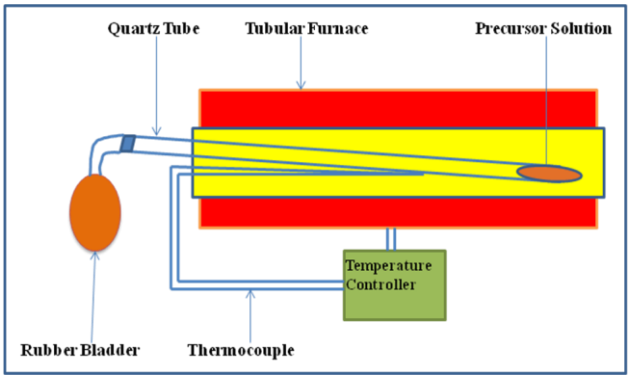

Fig. 1. Schematic diagram of single step pyrolysis unit.

The closed end of the quartz tube containing the catalyst and the precursor mixture is placed in a tubular furnace as shown in **Fig. 1** and heated up to 750 ^oC for 1.5 hours at a heating rate 20 ^oC per minute and then allowed to cool down to room temperature. At room temperature, the rubber bladder is removed from the quartz tube under the safety hood and the thick black MWCNTs deposited on the inner walls of the reactor quartz tube is taken out from the mid zone of the deposited area of the quartz tube . This experimental procedure is repeated for different concentration of ferrocene to xylene ratio. In this method neither carrier gas nor any substrates of pre-coated metal catalyst were employed for the synthesis of MWCNTs.

Purification of MWCNTs

The as-synthesised MWCNTs consists of metal particles (like Fe, Ni etc) as the catalyst residue depending on the type of catalyst used in the synthesis and carbonaceous impurities like amorphous carbon, fullerenes and carbon nanoparticles (CNP) will also be present. Hence purification of MWCNTs is very essential for wide range of potential applications. Various purification methods like chemical oxidation (gas phase oxidation, liquid phase oxidation, electrochemical oxidation) physical purification like filtration, centrifugation, solubilisation with functional groups, high temperature annealing, multi-step purification like HIDE-assisted multistep purification, microfiltration in combination with oxidation, sonication in combination with oxidation are available. Among these purifications, it has been claimed that air oxidation is quite superior to liquid-phase oxidative treatment [**21**]. Hence the as-synthesised MWCNTs were heated for 2 hours at 400 ^oC by keeping it in a quartz boat at ambient atmosphere using the tubular furnace. Before and after the air oxidation process the mass of the as-synthesised MWCNTs is measured. Usually the reduction in the mass of as-synthesised MWCNTs is observed, and is accounted for oxidation of the amorphous carbon to carbondioxide. The air oxidation of MWCNTs has its own limitations and metal particles (iron) originating from the catalyst cannot be removed directly; hence acid treatment is very essential. The usually used oxidants in

liquid phase oxidation are HNO_3 [**22-24**], H_2O_2 or a mixture of H_2O_2 & HCl [**25-27**], a mixture of H_2SO_4 and HCl, a mixture of H_2SO_4, HNO_3, $KMnO_4$ and NaOH [**28-31**]. In the present work, the air oxidised MWCNTs were treated with HCl of different molarity depending on the ferrocene to xylene ratio, higher the ratio, higher is the molarity of the HCl used to eliminate the iron particles originating from ferrocene.

Characterization

The crystalline phase of the as-synthesised MWCNTs was determined by X-ray powder diffraction (Bruker D8 Advanced Spectrometer) by using Cu Kα radiation. The morphological analysis was done by field emission scanning electron microscope (FESEM; QUANTA 250). Raman analysis (Horiba Jobin-LabRam-HR UV spectrometer) at ambient temperature with Argon laser as an excitation wavelength 514 nm was carried out for the crystallinity of MWCNTs as well as for identifying D band and G band and FT-IR (Bruker Tensor 27; OPUS 6.5) for functional group attachment and bond stretching analysis. The samples were prepared by grinding a little quantity of MWCNTs with KBr powder and pressing it to make a pellet. EDAX (Bruker) is also recorded to determine the chemical composition of the MWCNTs. The MWCNT's diameter and its distribution is studied using ImageJ software with the help of 2-dimensional SEM micrographs.

Results and discussion

Fig. 2 shows the XRD pattern of the purified MWCNTs. It is in accordance with JCPDS file no.75-1621. The major peak at about $2\theta \approx 26^o$ corresponds to (002) plane, also peaks corresponding to C(102) and C(004) confirms the synthesised material to be pure carbon with hexagonal structure. Peaks corresponding to oxides of iron were also found which could be attributed to the presence of iron in the catalyst.

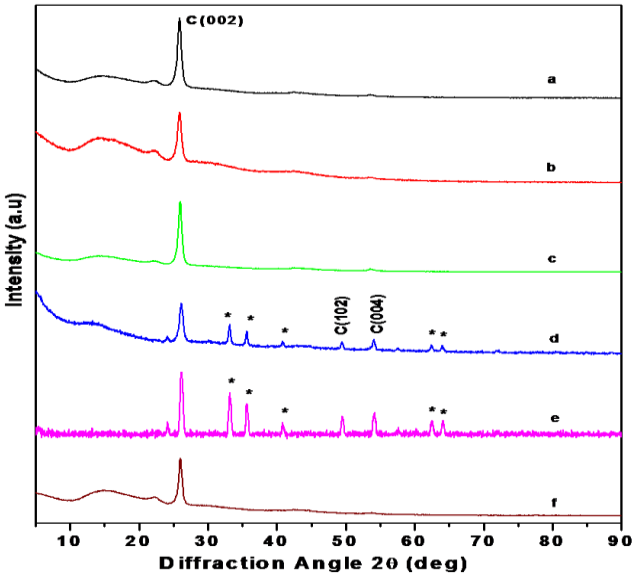

Fig. 2. XRD pattern of purified MWCNTs grown at (a) 20mg/ml; (b) 30mg/ml; (c) 40mg/ml; (d) 50mg/ml; (e) 60mg/ml (f) 70mg/ml. (***** indicates the iron oxide peaks).

Fig. 3 illustrates the field emission scanning electron micrographs (FESEM) of the purified MWCNTs synthesized at different ferrocene to xylene ratios. From the SEM micrographs we see that the external diameter of the MWCNTs is about 20 nm to 200 nm and its length is about 5 to 15 µm. The external diameter of the MWCNTs increases as the ferrocene to xylene ratio is increased. As the ferrocene content is increased in the precursor solution the agglomeration of iron particles leads the growth of the bigger diameter MWCNTs, bigger the agglomerate, larger will be the external diameter of MWCNT. This is very much evident from the micrographs.

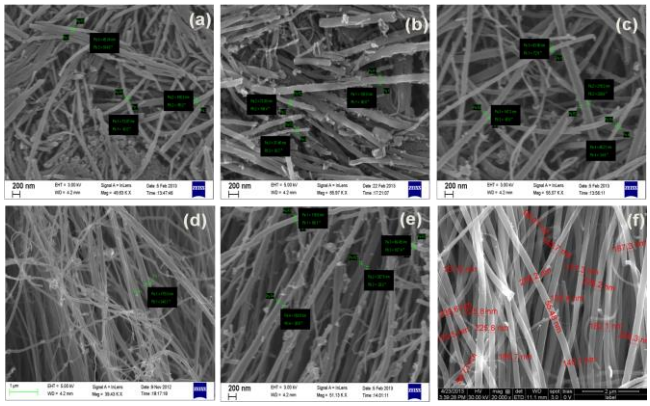

Fig. 3. Scanning electron microscope images of purified MWCNTs grown at (a) 20mg/ml; (b) 30mg/ml; (c) 40mg/ml; (d) 50mg/ml; (e) 60mg/ml; (f) 70mg/ml.

Fig. 4 shows the Raman spectra of the purified MWCNTs. Due to the presence of disordered amorphous carbon and double resonance effects in sp^2 carbon we see the D band at about 1350 cm^{-1} [**32**]. This band is not due to defects but due to the amorphous carbon in the tube walls [**33, 34**]. Also, due to the tangential vibrations of the graphitic carbon atoms we see the G band, at about 1580 cm^{-1}. A single peak at about 1580 cm^{-1} is graphitic in nature [**35**]. The 2D band, at about 2700 cm^{-1}, is due to two-phonon scattering around the K point of the Brillouin zone. The intensity of this peak depends strongly on the metallicity of the nanotube [**32**]. The ratio of intensities of D band and G band (I_D/I_G) is a measure of the extent of defects or functional groups present on the MWCNTs. **Fig. 5** gives the FT-IR spectra of the purified MWCNTs in the transmission mode in the range 400 to 4000 cm^{-1}. We find that the prominent peaks at 1328, 1387 (C=O), 1462 (CNT), 1638(C=C), 2362 (C-O), 2928(C-H_x), and 3434 (-OH) are noticed. Peak at 1462 cm^{-1} is attributed to MWCNT vibrational modes [**32**]. The peak at 2362 cm^{-1} corresponds to C-O bonds and the peaks between 2851-2925 cm^{-1} are consistent with C-H_x stretching vibrations of chemisorbed hydrogen of several types present in all MWCNTs [**36**]. **Fig. 6 (a, b, c, d, e** and **f)** depicts the histogram of the frequency of the occurrence with respect to the external diameter of MWCNTs. Using the ImageJ software the external diameter of the MWCNTs was measured using the 2-D SEM images and it is observed that as ferrocene to xylene ratio increases, the external diameter of MWCNTs also increases.

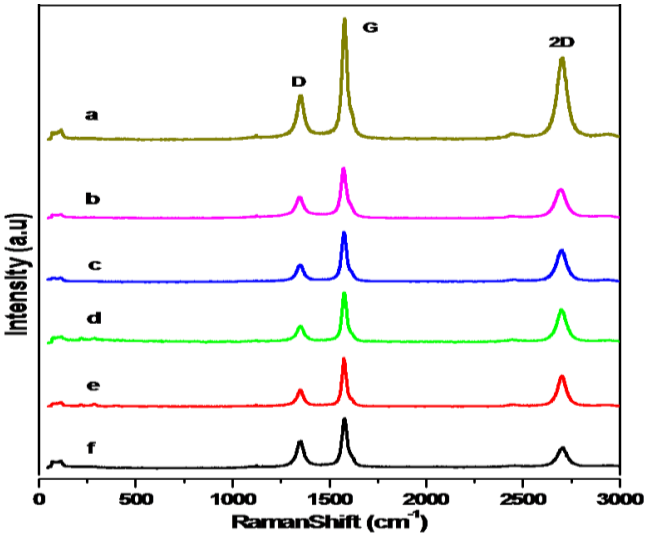

Fig. 4. Raman Spectra of purified MWCNTs grown using single step pyrolysis technique.

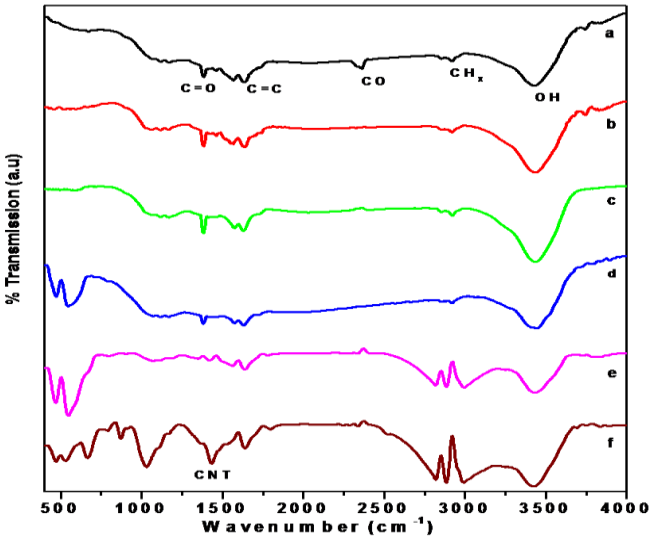

Fig. 5. FT-IR Transmission spectra of purified MWCNTs grown at (a) 20mg/ml; (b) 30mg/ml; (c) 40mg/ml; (d) 50mg/ml; (e) 60mg/ml; (f) 70mg/ml.

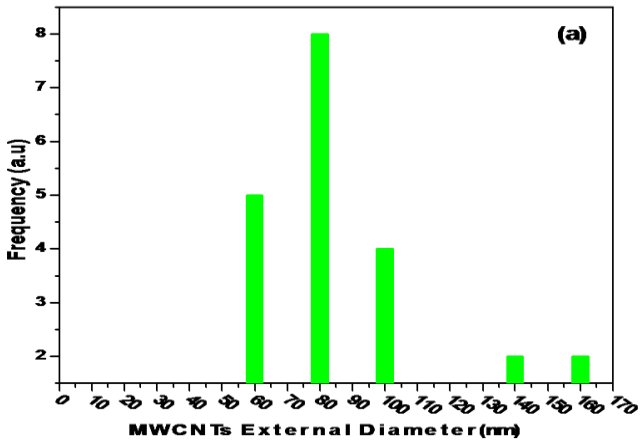

Fig. 6 (a). Histogram of MWCNTs external diameter against the frequency of occurrence of MWCNTs prepared at 20mg/ml (ferrocene to xylene ratio).

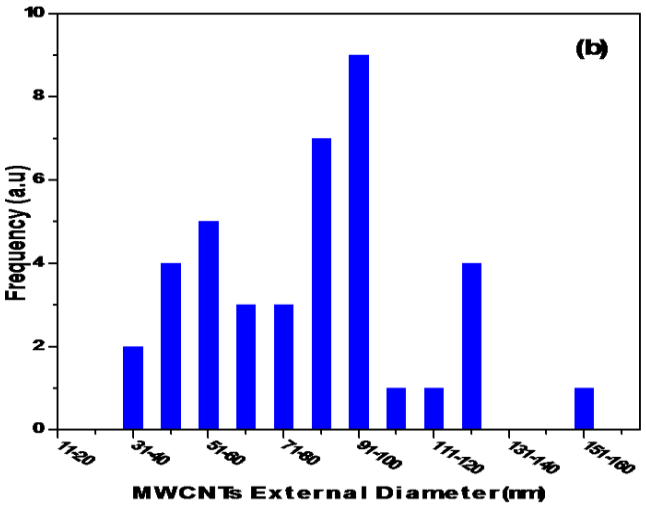

Fig.6b. Histogram of MWCNTs external diameter against the frequency of occurrence of MWCNTs prepared at 30mg/ml (ferrocene to xylene ratio).

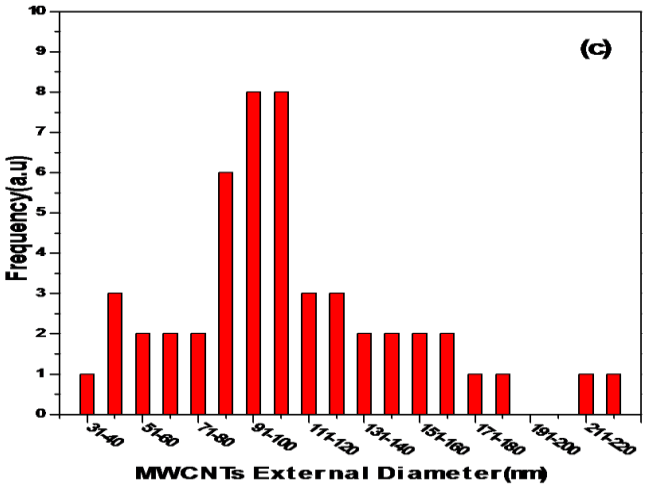

Fig.6 (c). Histogram of MWCNTs external diameter against the frequency of occurrence of MWCNTs prepared at 40mg/ml (ferrocene to xylene ratio).

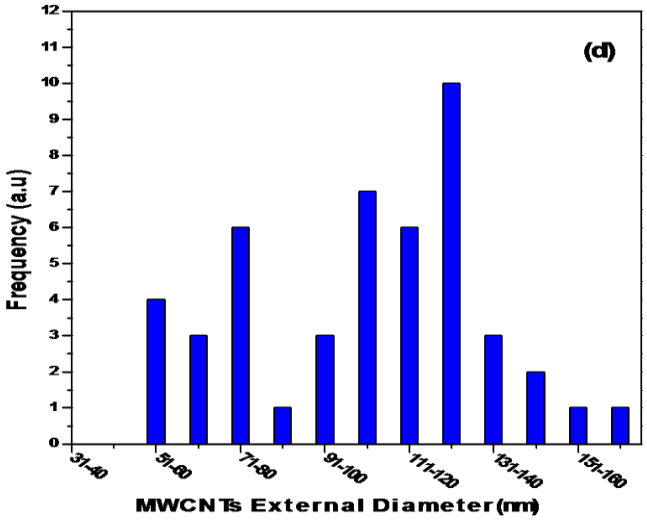

Fig.6 (d). Histogram of MWCNTs external diameter against the frequency of occurrence of MWCNTs prepared at 50mg/ml (ferrocene to xylene ratio).

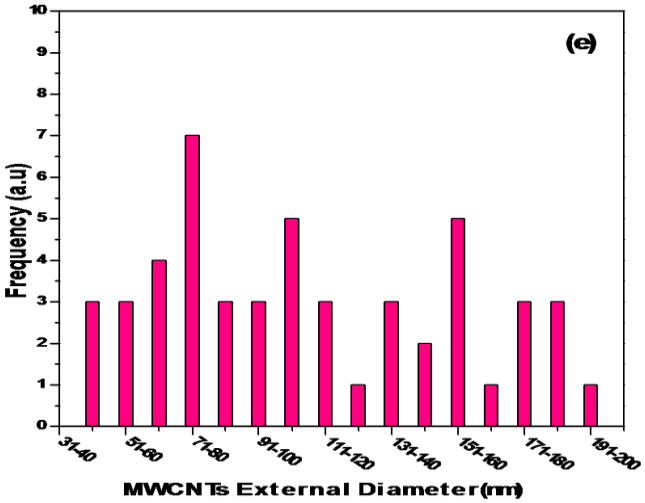

Fig. 6 (e). Histogram of MWCNTs external diameter against the frequency of occurrence of MWCNTs prepared at 60mg/ml (ferrocene to xylene ratio).

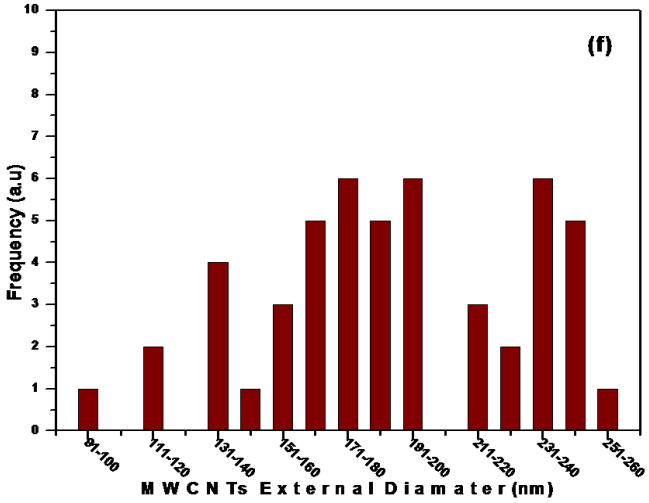

Fig. 6 (f). Histogram of MWCNTs external diameter against the frequency of occurrence of MWCNTs prepared at 70mg/ml (ferrocene to xylene ratio).

Conclusion

With the simple single step pyrolysis method MWCNTs were synthesised. These MWCNTs were characterised with XRD, FT-IR, Raman spectroscopy, FE-SEM. By measuring the external diameter of the MWCNTs from SEM images we found that the external diameter of the MWCNTs increases with the increase in the ferrocene content in the precursor solution. The agglomerated iron particles leads the growth of the bigger diameter MWCNTs, bigger the agglomerate, larger will be the external diameter of MWCNT. The higher concentrations of iron nanoparticles inside the MWCNTs can be useful for catalytic applications where these MWCNTs serve as scaffolds for iron nanoparticles as catalyst. Further optimization of other parameters is underway to speculate the maximum ferrocene content in the precursor solutions for the better growth of larger diameter MWCNTs.

Acknowledgements

One of the authors (BVMK) wishes to thank the administration of CeNSE, IISc, Bangalore, for providing the laboratory facilities and the UGC for providing the fellowship grant (TF CODE: KABA 095 TF 03), for pursuing the research work.

Reference

1. Iijima,; *Nature*, **1991**, *354*, 56. **DOI:** 10.1038/354056a0
2. Michael J.; Bronikowsk,; *Carbon*, **2006**, *44*, 2822. **DOI:** 10.1016/j.carbon.2006.03.022
3. Sejin Kyung.; Yonghyuk Lee.; Chanwoo Kim.; Junhee Lee.; Geunyoung Yeom.; *Thin Solid Films*, **2006**, *506–507*, 268. **DOI:** 10.1016/j.tsf.2005.08.325.
4. Li Chena.; Xiujiang Pang.; Guangshui Yua and Jianming Zhang.; *Adv. Mat. Lett*, **2010**, *1*, 75. **DOI:** 10.5185/amlett.2010.4117
5. Pradip Ghosh.; Tetsuo Soga.; Kaushik Ghosh.; Rakesh A. Afre.; Takashi Jimbo.; Yoshinori Ando.; *J Non-Crys. Solids*, **2008**, *354*, 4101. **DOI:** 10.1016/j.jnoncrysol.2008.05.053
6. Wei Zhaoa.; Hyun Sung Kimb.; Hyung Tae Kimc.; Jianghong Gongd and Ik Jin Kima,; *J Ceram Process Res*, **2011**, *12*, 392.
7. D. A. L. Almeida.; E. F. Antunes.; V. Q. da Silva.; M. R. Baldan.; N. G. Ferreira,; *J Solid State Electrochem*, **2013**, *17*, 1977. **DOI:** 10.1007/s10008-013-2052-0
8. Munir Mohammad.; Mohammad Bilal Khan.; Tauqir A. Sherazi.; Jose Anguita.; DamithaAdikaari,; *J Nano mater*, **2013**, *2013*, 1. **DOI:** 10.1155/2013/713583
9. Xiaodong Bai.; Dan Li Ye Wang.; Ji Liang,; *Tsinghua Science & Technology*, **2005**, *10*, 729. **DOI:** 10.1016/S1007-0214(05)70142-5
10. Shuo Bai.; Feng Li.; QuanHong Yang.; Hui-Ming Cheng.; JinBo Bai,; *Chem. Phys. Lett*., **2003,** *376*, 83. **DOI:** 10.1016/S0009-2614(03)00959-X
11. Yun Tack Lee.; Nam Seo Kim.; Jeunghee Park.; Jae Beom Han.; Young Sang Choi.; Hyun Ryu.; Hwack Joo Lee,; *Chem. Phys. Lett.*, **2003**, *372*, 853. **DOI:** 10.1016/S0009-2614(03)00529-3
12. F. H. Kaatz.; M. P. Siegal.; D. L. Overmyer.; P. P. Provencio.; D. R. Tallant,; Appl. *Phys. Lett*. **2006**, *89*, 241915 (1-3). **DOI:** 10.1063/1.2405847
13. Noor Asnida Asli.; Muhammad Salleh Shamsudin.; Suriani Abu Bakar.; Mohamad Rusop Mahmood.; Saifollah Abdullah,; *Int. J. Ind. Chem.* **2013**, *4*, 23. **DOI**: 10.1186/2228-5547-4-23
14. L. Tapasztó.; K. Kertész.; Z. Vértesy.; Z.E. Horváth.; A.A. Koós.; Z. Osváth.; Zs. Sárközi, Al. Darabont.; L.P. Biró,; *Carbon*, **2005**, *43*, 970. **DOI:** 10.1016/j.carbon.2004.11.048
15. Seyyed Shayan Meysami.; Antal A. Koos.; Frank Dillon.; Nicole Grabert.; *Carbon*, **2013,** *58*, 159. **DOI:** 10.1016/j.carbon.2013.02.041
16. Pitamber Mahanandia.; Karuna Kar Nanda,; *Nanotechnology*, **2008**, *19***,** 155602. **DOI:** 10.1088/0957-4484/19/15/155602
17. W. Z. Li.; S. S. Xie.; L. X. Qian.; B. H. Chang.; B. S. Zou.; W. Y. Zhou.; R. A. Zhao.; G. Wang,; *Science*, **1996**, *274*, 1701. **DOI:** 10.1126/science.274.5293.1701
18. M. Terrones.; N. Grobert.; J. Olivares.; J. P. Zhang.; H. Terrones.; K. Kordatos.; W. K. Hsu.; J. P. Hare.; P. D. Townsend.; K. Prassides.; A. K. Cheetham.; H. W. Kroto.; D. R. M. Walton,; *Nature*, **1997**, *388*, 52.
19. Govindaraju. A.; Rao. C.N.R.; *Pure Appl. Chem*., **2002**, *74*, 1571. **DOI:** 10.1351/pac200274091571
20. P. Mahanandiaa.; P.N. Vishwakarma.; K.K. Nanda.; V.Prasad.; K. Barai.; A.K. Mondal.; S. Sarangi.; G. K. Dey.; S.V. Subramanyam,; *Solid State Commun*, **2008**, *145*, 143. **DOI:** 10.1016/j.ssc.2007.10.020
21. Anil Suri.; Karl S. Coleman,; *Carbon*, **2011**, *49*, 3031. **DOI:** 10.1016/j.carbon.2011.03.023
22. Erik Dujardin.; Thomas W. Ebbesen.; Ajit Krishnan.; Michael M. J. Treacy,; *Adv. Mater*., **1998**,*10*,611.

23. A.G. Rinzler.; J. Liu, H.Dai1.; P. Nikolaev.; C.B. Huffman.; F.J. Rodr´ıguez-Mac´ıas.; P.J. Boul.; A.H. Lu.; D.Heymann.; D.T. Colbert.; R.S. Lee.; J.E. Fischer.; A.M.Rao.; P.C. Eklund.; R.E. Smalley,; *Appl. Phys. A*, **1998**, *67*, 29.
DOI: 10.1007/s003390050734
24. Hui Hu.; Bin Zhao.; Mikhail E. Itkis.; Robert C. Haddon,; *J. Phys. Chem. B*, **2003**, *107*, 13838**.**
DOI: 10.1021/jp035719i
25. Xinluo Zhao.; Masato Ohkohchi.; Sakae Inoue.; Tomoko Suzuki.; Takenori Kadoya.; Yoshinori Ando,; *Diam Relat Mater*., **2006**, *15*, 1098.
DOI: 10.1016/j.diamond.2005.11.002
26. Tomoko Suzuki.; Kenji Suhama.; Xinluo Zhao.; Sakae Inoue.; Noriyoshi Nishikawa.; Yoshinori Ando,; *Diam Relat Mater*., **2007**, *16*, 1116.
DOI: 10.1016/j.diamond.2006.11.006
27. Wang Y.; Shan H.; Hauge RH.; Pasquali M.; Smalley RE,; *J Phys Chem B.*, **2007,** *111*, 1249.
DOI: 10.1021/jp068229+
28. Liu J.; Rinzler AG.; Dai H.; Hafner JH.; Bradley RK.; Boul PJ.; Lu A.; Iverson T.; Shelimov K.; Huffman CB.; Rodriguez-Macias F.; Shon YS.; Lee TR.; Colbert DT.; Smalley RE,; *Science*, **1998**, *280*, 1253.
DOI: 10.1126/science.280.5367.1253
29. J.G. Wiltshire.; A.N. Khlobystov.; L.J. Li.; S.G. Lyapin.; G.A.D. Briggs.; R.J. Nicholas,; *Chem. Phys. Lett*., **2004**, *386*, 239–243.
DOI: 10.1016/j.cplett.2004.01.067
30. Yu Li.; Xiaobin Zhang.; Junhang Luo.; Wanzhen Huang.; Jipeng Cheng.; Zhiqiang Luo.; Ting Li.; Fu Liu.; Guoliang Xu.; Xiaoxing Ke.; Lin Li.; Herman J Geise,; *Nanotechnology*, **2004,** *15*, 1645.
DOI: 10.1088/0957-4484/15/11/047
31. Jin Zhang.; Hongling Zou.; Quan Qing.; Yanlian Yang. ;Qingwen Li.;Zhongfan Liu.; Xinyong Guo.; Zuliang Du,;, *J. Phys. Chem. B*, **2003**, *107*, 3712.
DOI: 10.1021/jp027500u
32. John H. Lehman.; Mauricio Terrones.; Elisabeth Mansfield.; Katherine E. Hurst.;Vincent Meunier,; *Carbon*, **2011**, *49*, 2581.
DOI: 10.1016/j.carbon.2011.03.028
33. S. Osswald.; E. Flahaut.; H. Ye.; Y. Gogotsi,; *Chem. Phys. Lett*., **2005**, *402*, 422**.**
DOI: 10.1016/j.cplett.2004.12.066
34. S. M. Bose.; S. Gayen.; S. N. Behera,; *Phys. Rev. B*, **2005**, *72*, 153402.
DOI: 10.1103/PhysRevB.72.153402
35. Ki Kang Kim.; Jin Sung Park.; Sung Jin Kim.; Hong Zhang Geng.; Kay Hyeok An.; Cheol-Min Yang.; Kentaro Sato.; Riichiro Saito.; Young Hee Lee,; *Phys. Rev. B*, **2007**, *76*, 205426.
DOI: 10.1103/PhysRevB.76.205426
36. Abha Misra.; Pawan K. Tyagi.; Padmnabh Rai.; D. S. Misra,; *J. Nanosci. Nanotechnol.* **2007**, *7*, 1820.
DOI: 10.1166/jnn.2007.723